

Estimating Radiant Fields in Flat Heterogeneous Photoreactors by the Six-Flux Model

A. Brucato

Università di Palermo, Dipartimento di Ingegneria Chimica dei Processi e dei Materiali (DICPM), Unità di Ricerca INCA
Palermo 2, Viale delle Scienze, 90128 Palermo, Italy

A. E. Cassano

INTEC, Universidad Nacional del Litoral y CONICET, Guemes 3450, 3000 Santa Fe, Argentina

F. Grisafi

Università di Palermo, Dipartimento di Ingegneria Chimica dei Processi e dei Materiali (DICPM), Unità di Ricerca INCA
Palermo 2, Viale delle Scienze, 90128 Palermo, Italy

G. Montante

Università di Bologna, Dipartimento di Ingegneria Chimica, Mineraria e delle Tecnologie Ambientali (DICMA), Viale
Risorgimento 2, 40136 Bologna

L. Rizzuti and G. Vella

Università di Palermo, Dipartimento di Ingegneria Chimica dei Processi e dei Materiali (DICPM), Unità di Ricerca INCA
Palermo 2, Viale delle Scienze, 90128 Palermo, Italy

DOI 10.1002/aic.10984

Published online September 15, 2006 in Wiley InterScience (www.interscience.wiley.com).

Heterogeneous photoreactor modeling is a task complicated by the integro-differential nature of the Radiation Transfer Equation (RTE) when scattering phenomena are important. In the present work, a novel "Six Flux Model" (SFM) is proposed, which may be regarded as a step forward with respect to the previously proposed "Two Flux Model" (TFM). In order to validate the newly proposed model, Monte Carlo simulations of an indefinite plane-slab photoreactor have been performed. As no simplifying assumptions are involved in this case, the information obtained may be regarded as "pseudo-experimental," and therefore compared with the predictions of both TFM and SFM models. Results show that the novel SFM is able to closely match the exact solution of the RTE better than the TFM, still retaining the TFM advantage of a simple closed-form solution, that is, ease of use, clearer effect of model parameters, and so forth. © 2006 American Institute of Chemical Engineers AIChE J, 52: 3882–3890, 2006

Keywords: heterogeneous photoreactor, radiant field, two-flux model, six-flux model, Monte Carlo

Introduction

Reliable tools for the design and development of heterogeneous photoreactors are required in order to successfully bring photo-catalytic processes to the industrial stage.

Modeling of photochemical reactors is a quite complex task. As a matter of fact, to the usual difficulties met in the modeling of conventional chemical reactors, other complications arise from the need to contemporaneously model the radiation flow field, which strongly affects reaction rates.

In general, when the chemical effects of radiant energy absorption are to be dealt with, the radiation field can be affected by the reactants' concentration field, which is affected by local reaction rates and, hence, in turn, by the radiation field,

Correspondence concerning this article should be addressed to A. Brucato at abrucato@dicpm.unipa.it.

thus resulting in a very complex modeling task. However, in the case of heterogeneous slurry photoreactors, the absorbing medium consists of solid particles that absorb and scatter light independently of the presence of reactants that are very often practically transparent to the radiation wavelengths involved in the activation of the photo-catalyst. In such cases, the radiation field is not coupled with the reactants' concentration field and can, therefore, be computed in advance. On the other hand, the radiation field always depends on the particle concentration field, which should be either experimentally assessed or simulated by suitable models. However, when catalyst particles are relatively small, particle concentration can often be considered uniform, thanks to the turbulent fluid motion usually encountered in such reactors.

Even when a uniform particle concentration exists, the modeling of radiant fields is still a very complex task, because of the complexity of the interaction between the radiation source and dispersed scattering-absorbing particles.

In order to accomplish this task, a solution of the Radiation Transfer Equation (RTE) would be required, but, due to the complexities of this equation, analytic solutions are allowed only for a few extremely simplified cases.^{1,2} For this reason, the following alternative approaches have been devised: (i) numerical solutions of the RTE (mainly based on the Discrete Ordinate Method), though its integro-differential nature makes this approach very complex³⁻⁷; (ii) numerical approaches based on Monte Carlo techniques,^{8,9} which enjoy a simpler model implementation but typically result into a heavier computational effort; (iii) strongly simplified radiation field models^{10,11} that, although approximate, give an immediate grasp and physical understanding of the role played by the key parameters on the whole process, which is often what is really needed for the design and development of industrial equipment.

Among this last approach, the two referenced works^{10,11} regard the case of plane slab photoreactors, and were named the Zero Reflectance Model (ZRM) and the Two Flux Model (TFM), respectively. The former is based on the assumption of absence of photon scattering by particles, while the latter assumes that when scattering occurs it takes place only in a perfect backward direction. Since the former overestimates the rate of photon absorption in the photoreactor, while the latter underestimates the same quantity, the two models give rise to predictions that bound the real behavior of photoreactors. As a consequence, for all cases where the photon absorption rates predicted by the two models do not differ too much, a reasonable estimate of the actual absorption rate as well as of the confidence limits, is achieved. For cases where the two models give rise to significantly different predictions, in order to devise a suitable averaging procedure, an indication about the extents of under- and over-estimation by the two models would be needed. However, so far only the ZRM has been experimentally validated, as the hypothesis of zero reflectance can be physically approached and also only simple-to-obtain transmittance data are required. On the other hand, the TFM relies on a perfect back-scatter hypothesis that cannot be physically reproduced. Moreover, integral quantitative reflectance data would be required in order to properly quantify the model deviations with respect to reality, and these are rather difficult to obtain.

In the present work, a novel simple Six Flux Model (SFM) is proposed, which is shown to be able to match quite closely

the exact solution of the RTE, while still retaining all the advantages of simplified models.

In order to validate the SFM, a Monte Carlo approach is applied to the case of an indefinite plane-slab photoreactor. In this way, integral transmittance and reflectance data are obtained, which do not rely on any simplifying assumption on the scattering phase function and can, therefore, be regarded as "pseudo-experimental" data to be compared with predictions of the previous ZRM and TFM models and of the proposed SFM model. Finally, the deviations of all models with respect to the (impossible) exact solution of the RTE are suitably quantified and discussed.

Monte Carlo Approach

In order to obtain data suitable for simplified models validation, a statistical approach, on the grounds of a Monte Carlo procedure, was used. The history of a statistically meaningful number of photons traveling inside a flat-type solid-liquid photoreactor was obtained under the hypothesis of uniformly distributed catalyst particles of the same size and a uniformly irradiated, indefinitely wide, slab photoreactor of thickness L . Under the above assumptions, due to symmetry considerations, the only direction in which changes can take place is that of reactor depth.

Fundamentals of the Monte Carlo technique are well known.¹² In the fields of photochemistry and photocatalysis, the Monte Carlo technique has been applied by Spadoni⁸ and Pasquali and Santarelli⁹ in investigations concerning photoassisted reactions.

The approach here employed allows the determination of the transmitted and reflected radiative fluxes, G_L and g_o , as well as of the Local Volumetric Rate of Photon Absorption (LVRPA), that is, the number of photons absorbed per unit reactor volume and unit time, a very important parameter needed to link radiation distribution to local reaction kinetics.¹³

In order to describe the entire approach, let us follow the fate of a photon, starting from its first entrance in the photoreactor volume, until it either escapes from the photoreactor or is absorbed by a photocatalyst particle.

Assuming that the photon under consideration has just survived a scattering event inside the reactor, it is possible to calculate the length traveled by the photon before a further event (scattering or absorption) occurs. This length clearly depends on the probability of the photon to collide with a particle inside the photoreactor. This probability can be obtained by generating a random number, R_1 , so that, as the cumulative distribution of the probability density follows an exponential law, the length traveled by the photon between two subsequent interactions can be computed as:

$$l_i = -\lambda_0 \ln R_1 \quad (1)$$

where λ_0 is the mean free path of photons, which is easily related to particle size and concentration as specified later on (Eq. 7).

If x_{i-1} is the coordinate at which the last interaction occurred (where x is distance from reactor front plane), the depth of the new interaction is simply given by:

$$x_i = x_{i-1} + l_i \cos \theta_i = x_{i-1} - \lambda_0 \ln R_1 \cos \theta_i \quad (2)$$

where θ_i is the angle between the photon traveling direction and the x axis direction.

Clearly, a result of $x_i < 0$ would mean that the photon actually left the photoreactor from the front wall, while a result of $x_i > L$ would mean that the photon escaped from the photoreactor rear wall. In all other cases, a new photon-particle interaction occurs at the specified location.

If this is the case, another random number, R_2 , is generated and compared with the albedo, R . The photon is considered to be absorbed if $R_2 > R$, while it is scattered if $R_2 < R$.

In this last case, the scattering angle θ_{i+1} , defined by the latitude angle φ_{i+1} and the longitude angle ω_{i+1} , must be determined. To calculate the latitude angle, it is necessary to adopt a suitable phase function. There is no general consensus on the best phase function to adopt, due to the fact that it depends on particle size, shape, and surface properties. Therefore, different phase functions should probably be adopted for different systems. In this work, the well-known and theoretically sound "diffusely reflecting large sphere" phase function¹⁴ was considered suitable. It is described by the following relationship:

$$\Phi(\varphi) = \frac{8}{3\pi} (\sin \varphi - \varphi \cos \varphi) \quad (3)$$

According to this, it follows that:

$$\begin{aligned} R_3 &= \int_0^\varphi p(\varphi) d\varphi = \int_0^\varphi \frac{\sin(\varphi)}{2} \Phi(\varphi) d\varphi \\ &= \frac{1}{6\pi} (4\varphi_{i+1} + 2\varphi_{i+1} \cos 2\varphi_{i+1} - 3 \sin 2\varphi_{i+1}) \end{aligned} \quad (4)$$

where R_3 is a random number. The latitude angle φ_{i+1} can be obtained from Eq. 4.

Since the same probability can be assigned to all directions,⁸ the longitude angle ω_{i+1} is simply obtained as:

$$\omega_{i+1} = 2\pi R_4 \quad (5)$$

The knowledge of φ_{i+1} and ω_{i+1} allows the calculation of θ_{i+1} , the angle of scattering relative to the x direction, by a geometric relationship:

$$\theta_{i+1} = \cos \varphi_{i+1} \cos \theta_i + \sin \varphi_{i+1} \cos \omega_{i+1} \sin \theta_i \quad (6)$$

For a new photon, the procedure starts when the photon enters the reactor, that is, $x_0 = 0$ and $\theta = \theta_0$, where θ_0 is the angle between the direction of the incoming radiation and the x axis. In the present work, θ_0 was always set to zero, that is, a uniform orthogonal irradiation was considered. The procedure ends when the photon is either absorbed or escapes from the photoreactor.

In practice, the input parameters for the procedure here employed were:

- (a) the photocatalyst albedo $R = \sigma/(\kappa + \sigma)$;

- (b) the optical thickness, L/λ_0 , given by the ratio between photoreactor depth, L , and the photon mean free path length, λ_0 ;

- (c) the number of photons, n .

Values of g_0 and G_L , normalized with respect to the incoming flux G_0 , were simply obtained by counting all the photons leaving the photoreactor from the front or the rear wall, respectively, and dividing these numbers by the total number of photons, n .

In order to obtain the local volumetric rate of photon absorption (LVRPA), the photoreactor depth was suitably discretized into a number of slices of depth Δx . The average (normalized) LVRPA in each slice was obtained by simply counting the number of absorption events that occurred in the slice, and dividing this number by G_0 and by $\Delta x/L$.

This procedure has been utilized to perform a large number of simulations. In all these simulations, the direction of the photon initial incidence angle was normal to the photoreactor wall, as the first intent of this work was that of simulating this simple radiation arrangement. The calculation code was written in FORTRAN and run on a personal computer by using the internal random numbers generator.

As regards the number of photons, all runs were performed following the fate of 10^6 photons. This value was chosen after the same runs were carried out by varying only the number of photons from 10^2 to 10^7 . The results were found to not change any more above the value of 10^5 . However, the value of 10^6 was chosen as a conservative one, as even with a common PC the CPU times never exceeded a few seconds.

If we suppose that the MC procedure here used well represents the real phenomena occurring inside the photoreactor, then the used photons number is so high that a simulation run can be considered as a good reproduction of a real experiment. In the data collection, the parameters R and L/λ_0 were varied. As regards R , the entire 0-1 range has been explored; while the values of L/λ_0 ranged from 0.5 to 10. This second range was chosen as being representative of real operative conditions.

For instance, it is possible to refer to the case of water dispersed commercial TiO_2 particles, which are mainly present in the slurry as aggregates of 0.5-1 μm . For dilute suspensions of "large" opaque particles, λ_0 has been shown¹⁰ to be related to the physical characteristics of the suspension by the simple relationship:

$$\lambda_0 = \frac{\rho_p D_p \alpha / \beta}{m} \quad (7)$$

Assuming for the aggregates an apparent density of 3000 Kg/m^3 , spherical shape ($\alpha/\beta = 0.667$), $D_p = 0.75 \mu\text{m}$, and $m = 0.3 \text{Kg/m}^3$, a value close to the critical value found by Augugliaro,¹⁵ λ_0 computed on the basis of Eq. 7 is 0.005 m and, therefore, a L/λ_0 variable in the range 0.5-10 corresponds to reactor thickness of 2.5-50 mm.

Comparison Monte Carlo—Two Flux Model

In this section the "experimental" data obtained by performing MC simulations are compared with the Two Flux Model proposed by Brucato and Rizzuti.¹¹ The comparison is shown in Figures 1 and 2, where values of g_0/G_0 and G_L/G_0 , calculated

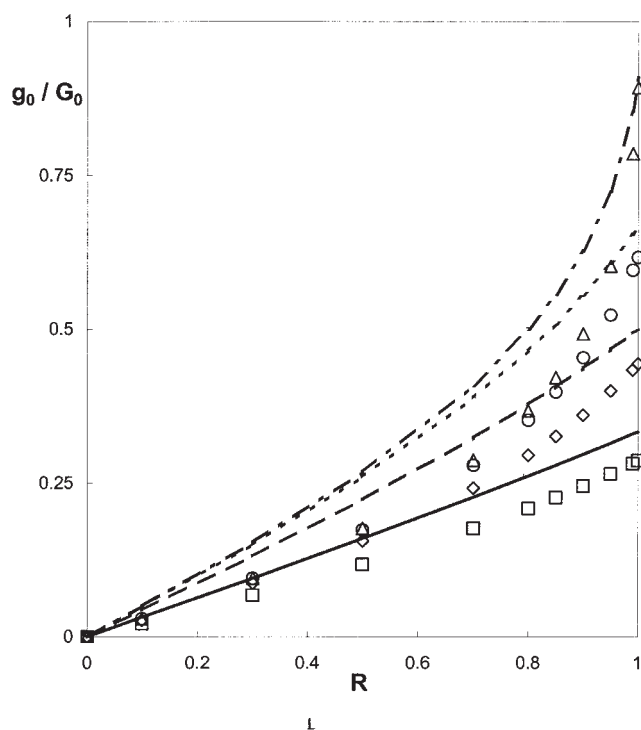


Figure 1. Comparison of the reflected radiant energy predicted by TFM (lines) with MC data (symbols).

$L/\lambda_0 = 0.5$ — \square ; $L/\lambda_0 = 1.0$ - - - \diamond ; $L/\lambda_0 = 2.0$ \circ ; $L/\lambda_0 = 10$ - · - · \triangle .

by the TFM equations and obtained by MC simulations, are plotted versus the albedo R , for several values of L/λ_0 .

A scrutiny of Figure 1 shows that the TFM always overestimates the value of g_0/G_0 . A better agreement is clearly observed for G_L/G_0 , in particular for large values of L/λ_0 , and for small values of the albedo, as found also by Li Puma and Yue.¹⁶ The relative absorbed photon flux can be easily obtained as the complement to one of the sum of the transmitted and reflected fluxes. It is plotted in Figure 3 for the same data of the two previous figures. Clearly, the absorption flux is somewhat underestimated, especially at large values of the albedo R , as predicted by the same authors.¹¹

Six Flux Model

In order to overcome the limitations observed with TFM, a new simple model was devised, where photons are supposed to be scattered in any of the six principal directions with respect to the incoming radiation. In this case, six different photon fluxes have to be considered, hence the name Six-Flux Model (SFM). The model bears some similarity with the “random walk model,” a numerical procedure based on a similar initial approach, and proposed by Yokota.¹⁷ However, in this work, only numerical solutions were reported; while in the present work, through the solution of differential photon balances, analytical solutions are obtained, from which transmitted and reflected photon fluxes can be calculated once the optical properties of the suspension are known.

The SFM relies on the following assumptions:

(a) infinitely wide slab of thickness L ;

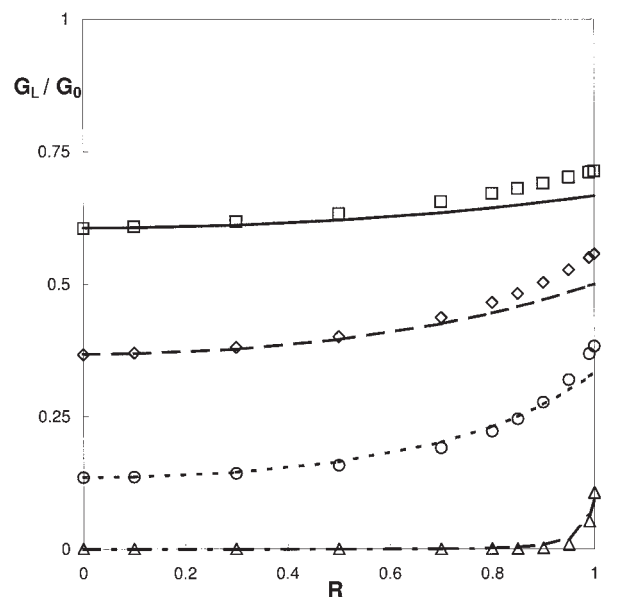


Figure 2. Comparison of the transmitted radiant energy predicted by TFM (lines) with MC data (symbols).

$L/\lambda_0 = 0.5$ — \square ; $L/\lambda_0 = 1.0$ - - - \diamond ; $L/\lambda_0 = 2.0$ \circ ; $L/\lambda_0 = 10$ - · - · \triangle .

(b) geometric optics holds true (hence, large and largely spaced particles);

(c) random particles distribution inside the space considered;

(d) the fluid does not absorb any radiation;

(e) there is no emission by the heterogeneous system;

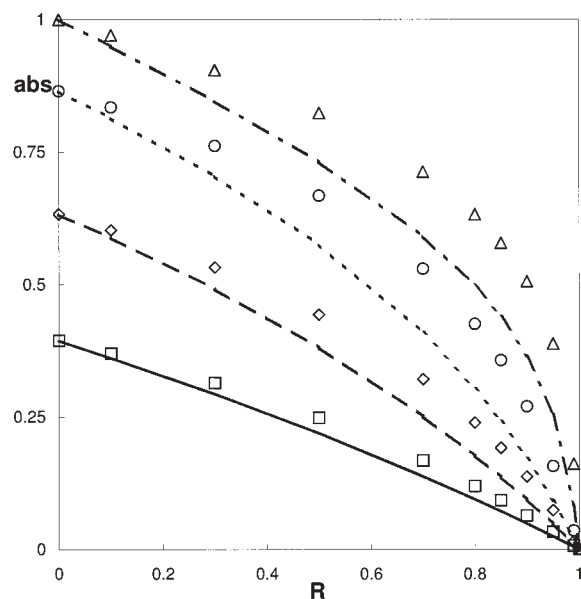


Figure 3. Comparison of the absorbed radiant energy predicted by TFM (lines) with MC data (symbols).

$L/\lambda_0 = 0.5$ — \square ; $L/\lambda_0 = 1.0$ - - - \diamond ; $L/\lambda_0 = 2.0$ \circ ; $L/\lambda_0 = 10$ - · - · \triangle .

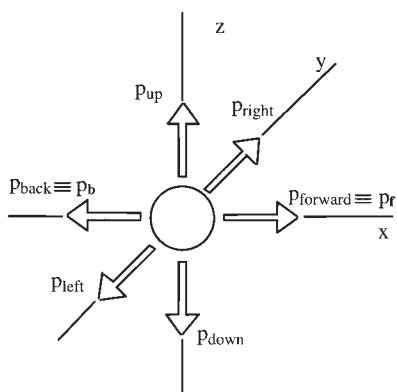


Figure 4. Six Flux Model scattering directions.

(f) when a photon hits a particle, only scattering or absorption occurs; the scattering probability is given by the catalyst albedo R ;

(g) the scattering event can occur only along the six directions of the Cartesian coordinates, as depicted in Figure 4;

(h) for symmetry considerations, the probability of scattering along any of the four directions of the plane normal to the incoming direction is the same; with regard to Figure 4, this means that

$$p_{up} = p_{down} = p_{right} = p_{left} \equiv p_s \quad (8)$$

From assumptions f, g, and h, it clearly arises that:

$$1 = abs + Rp_b + Rp_f + 4Rp_s \quad (9)$$

Symmetry considerations immediately lead to:

$$g_{up} = g_{down} = g_{right} = g_{left} \equiv g_s \quad (10)$$

By defining a control volume $\Delta x \Delta y \Delta z$ and a forward photon flux G , as in Figure 5, on the basis of the considerations reported by Brucato and Rizzuti,¹¹ the following photon balance can be written:

$$\begin{aligned} \Delta y \Delta z G|_{x+\Delta x} &= \Delta y \Delta z G|_x - \Delta y \Delta z G(1-R)n_p a_p \Delta x \\ &\quad - \Delta y \Delta z GR(p_b + 4p_s)n_p a_p \Delta x + \Delta y \Delta x g_d R p_u n_p a_p \Delta z \\ &\quad + \Delta y \Delta x g_u R p_d n_p a_p \Delta z + \Delta x \Delta z g_l R p_r n_p a_p \Delta y \\ &\quad + \Delta x \Delta z g_r R p_l n_p a_p \Delta y + \Delta y \Delta z g_b R p_f n_p a_p \Delta x \quad (11) \end{aligned}$$

where n_p is the number of particles per unit volume, a_p is the projected area of one particle, and pedices u, d, r , and l stand for *up, down, right*, and *left*, respectively.

Dividing by $\Delta x \Delta y \Delta z$ and making Δx vanishingly small, one obtains:

$$\frac{dG}{dx} = \frac{1}{\lambda_0} [G(Rp_f - 1) + 4g_s Rp_s + g_b Rp_b] \quad (12)$$

where:

$$\lambda_0 = \frac{1}{n_p a_p} \quad (13)$$

In the same way by performing a photon balance in the backward direction one obtains:

$$\frac{dg_b}{dx} = \frac{1}{\lambda_0} [(1 - Rp_f)g_b - 4g_s Rp_s - GRp_b] \quad (14)$$

The unknowns of Eqs. 12 and 14 are G , g_b , and g_s . A third independent equation is needed for their determination. To this aim, the photon balance along the y direction can be written in the same way as for the x direction, resulting in:

$$\frac{dg_{left}}{dy} = n_p a_p [-g_s(1 - Rp_f - Rp_b - 2Rp_s) + g_b Rp_s + GRp_s] \quad (15)$$

Clearly, for symmetry considerations, the assumption of an infinitely large system results in:

$$\frac{dg_{left}}{dy} = \frac{dg_{right}}{dz} = 0 \quad (16)$$

Hence:

$$g_s = \frac{Rp_s}{(1 - Rp_f - Rp_b - 2Rp_s)} (G + g_b) \quad (17)$$

Substitution of g_s in Eqs. 12 and 14 gives rise to the following ODE system:

$$\frac{dG}{dx} = \frac{a}{\lambda_0} (R_{corr} g_b - G) \quad (18)$$

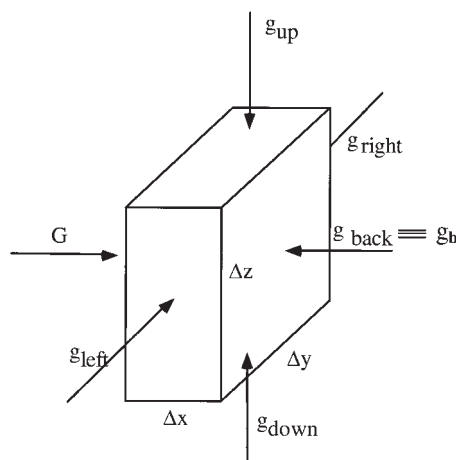


Figure 5. Differential model for the radiant energy balance.

$$\frac{dg_b}{dx} = \frac{a}{\lambda_0} (g_b - R_{corr}G) \quad (19)$$

with:

$$R_{corr} = \frac{b}{a} \quad (20)$$

$$a = 1 - Rp_f - \frac{4R^2p_s^2}{(1 - Rp_f - Rp_b - 2Rp_s)} \quad (21)$$

$$b = Rp_b + \frac{4R^2p_s^2}{(1 - Rp_f - Rp_b - 2Rp_s)} \quad (22)$$

As can be seen, Eqs. 18 and 19 practically coincide with the similar equations obtained for the TFM by Brucato and Rizuti^{10,11} by simply substituting R_{corr} to R .

Also, the ODE system has to be solved with the same boundary conditions:

$$\text{B.C.1 } G = G_0 \quad \text{when } x = 0$$

$$\text{B.C.2 } g_b = 0 \quad \text{when } x = L \quad (23)$$

Therefore, by introducing the “corrected” values for the main parameters, R_{corr} and λ_{Rcorr} , the final equations obtained for the TFM can be applied to the SFM as well, that is:

$$G = \frac{G_0}{(1 - \gamma)} \exp\left(-\frac{x}{\lambda_{Rcorr}}\right) \left[1 - \gamma \exp\left(-\frac{2x}{\lambda_{Rcorr}}\right)\right] \quad (24)$$

$$g_b = \frac{G_0}{R_{corr}(1 - \gamma)} \left[(1 - \sqrt{1 - R_{corr}^2}) \exp\left(-\frac{x}{\lambda_{Rcorr}}\right) - \gamma(1 + \sqrt{1 - R_{corr}^2}) \exp\left(-\frac{x}{\lambda_{Rcorr}}\right) \right] \quad (25)$$

with:

$$\gamma = \frac{1 - \sqrt{1 - R_{corr}^2}}{1 + \sqrt{1 - R_{corr}^2}} \exp\left(-\frac{2L}{\lambda_{Rcorr}}\right) \quad (26)$$

$$\lambda_{Rcorr} = \frac{\lambda_0}{a \sqrt{1 - R_{corr}^2}} \quad (27)$$

The transmitted and reflected radiative fluxes can be obtained by imposing $x = L$ and $x = 0$ in Eqs. 24 and 25, respectively:

$$G_L = \frac{G_0}{(1 - \gamma)} \left(\frac{2 \sqrt{1 - R_{corr}^2}}{1 + \sqrt{1 - R_{corr}^2}} \right) \exp\left(-\frac{L}{\lambda_R}\right) \quad (28)$$

$$g_{b,0} = g_0 = \frac{G_0}{R_{corr}} \left[1 - \frac{(1 + \gamma)}{(1 - \gamma)} \sqrt{1 - R_{corr}^2} \right] \quad (29)$$

The LVRPA can be obtained from a photon balance on the small volume comprised between x and $x + dx$:

$$LVRPA = -\frac{dG}{dx} + \frac{dg_b}{dx} \quad (30)$$

By substituting Eqs. 24 and 26 into Eq. 30, one obtains:

$$LVRPA = \frac{G_0}{\lambda_{Rcorr}R(1 - \gamma)} \cdot [(R_{corr} - 1 + \sqrt{1 - R_{corr}^2})e^{-x/\lambda_{Rcorr}} + \gamma(R_{corr} - 1 - \sqrt{1 - R_{corr}^2})e^{x/\lambda_{Rcorr}}] \quad (31)$$

Comparison Six Flux Model—Monte Carlo

In order to compare the SFM results with the exact solution, as approximated by the Monte Carlo procedure, the three parameters p_b , p_f , and p_s need to be specified. This was done by a trial and error best fit procedure that was applied for a given albedo value ($R = 0.5$), resulting in the following set of values for the three parameters: $p_b = 0.71$, $p_f = 0.11$, and $p_s = 0.044$, for the phase function adopted here (Eq. 3).

Clearly, the SFM could be considered as being well validated if not only a good agreement was achieved in the selected case of $R = 0.5$, but if the same set of parameters resulted in good agreement also at all other values of the albedo R .

In Figure 6 the photon flux reflected by the front photoreactor wall as predicted by SFM and MC is reported. As can be seen, a striking agreement is found for all R values, irrespective of the reactor optical thickness L/λ_0 parameter, which was varied in an ample range. If one compares the SFM results of Figure 6 with the TFM results reported in the germane Figure 1, the model accuracy improvement when using SFM over TFM is apparent.

In Figure 7, the normalized transmitted photon flux obtained by SFM and MC is reported. Again, a remarkable agreement between SFM results and the exact solution (MC data) is observed. Also, the comparison with Figure 2 clearly shows the extent of the improvement of SFM over TFM.

Not surprisingly, the absorbed photon flux is also found to be very well predicted at all R and L/λ_0 values, as shown in Figure 8, which is to be compared with Figure 3 for SFM/TFM assessment.

It is worth noting that the above remarked improvement of SFM predictions with respect to those obtained by TFM does not involve any significant additional computational burden, as the equations involved in the computation are actually the same, with the only difference of employing “corrected” values for R and L/λ_0 , as specified by Eqs. 20 and 27.

As previously mentioned, among the important quantities for photoreactor modeling purposes, the LVRPA is directly linked to the local photoreaction rates and therefore provides a more detailed description of photoreactor behavior, thus performing a more severe test of the model. This comparison is reported in Figure 9 for L/λ_0 equal to 2 and two rather extreme values of R (0.2 and 0.9). In Figure 10, the same information is reported for the case of L/λ_0 equal to 10. In these figures, the dimensionless LVRPA, that is, the LVRPA divided by the mean value in the hypothesis of complete absorption inside the reactor (G_0/L), is reported versus the position inside the reactor.

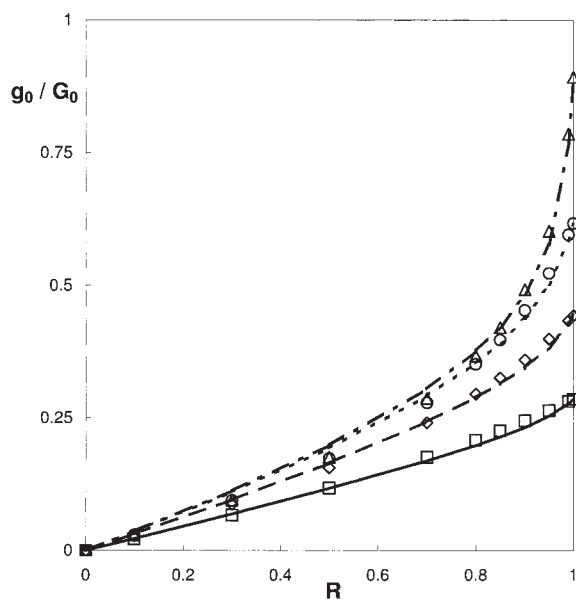


Figure 6. Comparison of the reflected radiant energy predicted by SFM (lines) with MC data (symbols).

$L/\lambda_0 = 0.5$ — \square ; $L/\lambda_0 = 1.0$ - - - \diamond ; $L/\lambda_0 = 2.0$ \circ ;
 $L/\lambda_0 = 10$ - · - · \triangle .

Observation of these figures leads to the conclusion that the agreement between the SFM and the exact (MC) results is excellent for the low albedo value ($R = 0.2$), independently of L/λ_0 . For the high albedo value ($R = 0.9$) the exact solution shows a relative maximum of LVRPA, a feature not predicted

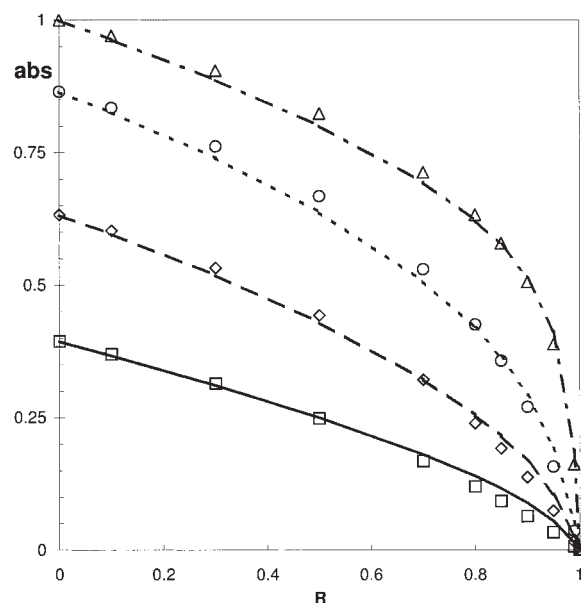


Figure 8. Comparison of the absorbed radiant energy predicted by SFM (lines) with MC data (symbols).

$L/\lambda_0 = 0.5$ — \square ; $L/\lambda_0 = 1.0$ - - - \diamond ; $L/\lambda_0 = 2.0$ \circ ;
 $L/\lambda_0 = 10$ - · - · \triangle .

by SFM. Notably, a similar local maximum had already been obtained in DOM simulations⁴ and is, therefore, likely to be a real radiation field feature. Its location is very close to the photon inlet wall, and it is dependent on L/λ_0 , being, in particular, closer to the wall, the higher the L/λ_0 . Although for the sake of clarity, the relevant data are not reported in Figures 9

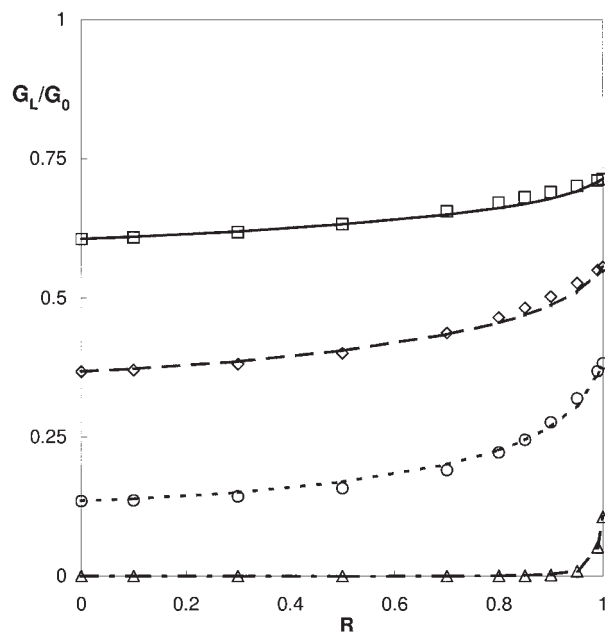


Figure 7. Comparison of the transmitted radiant energy predicted by SFM (lines) with MC data (symbols).

$L/\lambda_0 = 0.5$ — \square ; $L/\lambda_0 = 1.0$ - - - \diamond ; $L/\lambda_0 = 2.0$ \circ ;
 $L/\lambda_0 = 10$ - · - · \triangle .

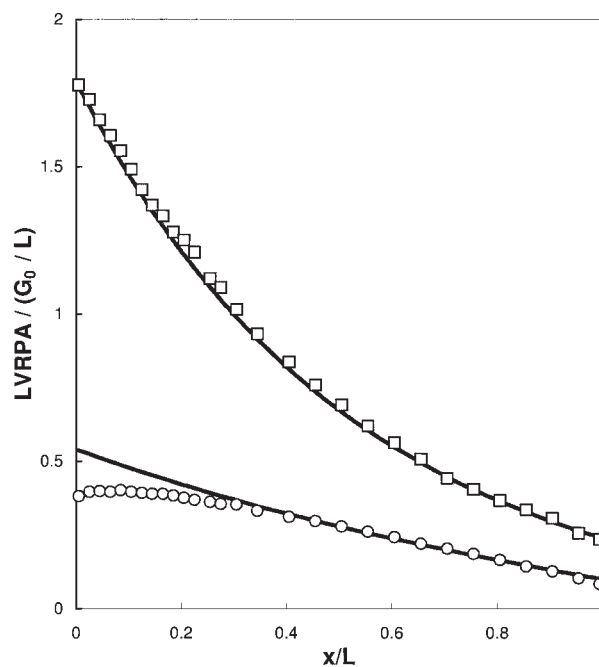


Figure 9. Normalized LVRPA.

Comparison. Case $L/\lambda_0 = 2$ Lines: SFM predictions; symbols: MC data. Squares: $R = 0.2$, circles: $R = 0.9$.

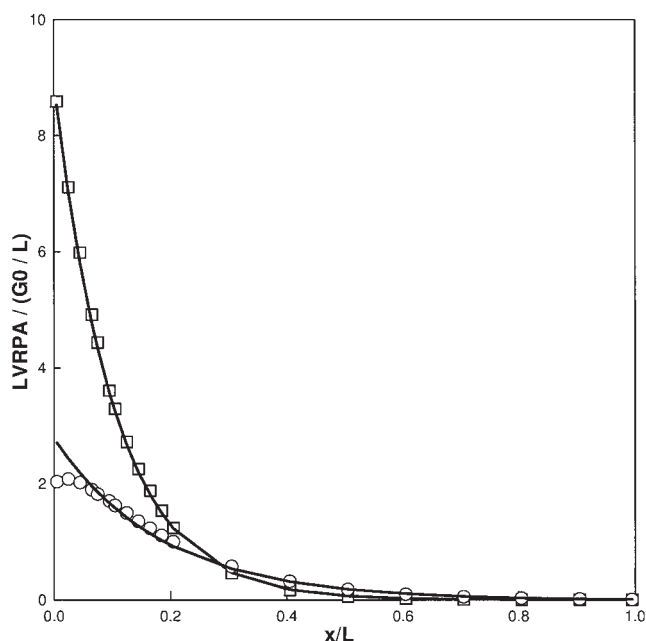


Figure 10. Normalized LVRPA.

Comparison. Case $L/\lambda_0 = 10$. Lines: SFM predictions; symbols: MC data. Squares: $R = 0.2$, circles: $R = 0.9$.

and 10, it has been found that for $L/\lambda_0 = 2$ the maximum appears for $R = 0.6$, while for $L/\lambda_0 = 10$ it appears for $R = 0.8$.

None of these features is reproduced by the SFM. It must be noted, however, that the disagreement is confined to high albedo values, and that it concerns only the very first layers of the photoreactor thickness. In particular, for $L/\lambda_0 = 2$, that is, for a situation certainly far away from any real photoreactor due to the large photon flux lost by transmission, the two approaches lead to significant differences over a thickness of about 30% of the total reactor depth. For $L/\lambda_0 = 10$, a much more realistic situation, this percentage drops to only 5%. Clearly the agreement is very good in all the rest of the photoreactor space. It is also worth noting that the most important parameter of photocatalytic processes is the total radiant flux absorbed, a quantity for which the SFM results have already been shown to be in very good agreement with MC results. This implies that the integral value of LVRPA is well reproduced by SFM, though as concerns the accuracy of the details of its spatial distribution there may be slight differences.

Conclusions

In the present work a simple approach, based on lumping the radiant field over six directions and named the Six Flux Model (SFM), was proposed. It may be regarded as a development of the previously introduced Two-Flux Model (TFM).

In order to validate the newly proposed model, Monte Carlo simulations of an indefinite plane-slab photoreactor were conducted, assuming for the phase function that pertaining to large, diffusely reflecting spheres. As no simplifying assumptions were involved, the information obtained in this way practically coincides with the exact solution of the RTE (as obtained from the analytical solution, had this been viable).

Monte Carlo results were first compared with ZRM and

TFM model predictions, resulting in reasonable agreement, though with the discrepancies expected on the basis of qualitative deductions.

On the contrary, the novel Six Flux Model was found to be able to closely match the exact solution of the RTE over the entire range of particle albedo, as far as photon losses by bed transmission and reflection are concerned. The spatial distribution of the photon absorption rate is also very well reproduced, with the only exception of the front reactor region in the case of very large particle albedo, where the SFM appears unable to reproduce the relative absorption maxima observed in the MC simulation results.

Considering that photocatalyst particles are unlikely to show large albedo with the photons of interest for their photo-excitation, the above slight discrepancies are not expected to affect in any way the practical utilization of SFM.

It is finally worth noting that SFM is able to provide information very close to the exact RTE solution, while still retaining all the advantages (effortless results, ease of grasping the physics of the phenomena) of more simplified models like the TFM.

Acknowledgments

This research was supported by a grant to INCA "Consorzio Interuniversitario La Chimica per l'Ambiente" on Legge 488 funds, Research Project 3: "Rimozione di inquinanti mediante processi a membrana e fotocatalitici."

Notation

- a = dimensionless parameter defined in Eq. 20
- a_p = projected area of one catalyst particle [m^2]
- abs = absorbed photons flux [$\text{einstein s}^{-1} \text{m}^{-2}$]
- b = dimensionless parameter defined in Eq. 21
- D_p = catalyst particle diameter [m]
- g_b = backward radiant flux [$\text{einstein s}^{-1} \text{m}^{-2}$]
- G = forward radiant flux [$\text{einstein s}^{-1} \text{m}^{-2}$]
- L = photoreactor thickness in the radiant flux direction [m]
- $LVRPA$ = Local Volumetric Rate of Photon Absorption [$\text{einstein s}^{-1} \text{m}^{-3}$]
- m = catalyst concentration [Kg m^{-3}]
- n = number of photons
- n_p = number of particles per unit volume [m^{-3}]
- $P_{f,b,s}$ = probabilities (forward, backward, sideward)
- R = albedo (intrinsic catalyst reflectance)
- R_{corr} = dimensionless parameter defined in Eq. 24
- R_1, R_2, R_3, R_4 = random numbers in 0-1 range
- x, y, z = cartesian coordinates, the yz plane is parallel to reactor walls

Greek letters

- α = shape factor for particles volume (part. volume = αd_p^3)
- β = shape factor for part. projected area (part. projected area = βd_p^2)
- γ = dimensionless parameter defined in Eq. 26
- φ = latitude angle [rad]
- κ = volumetric absorption coefficient [m^{-1}]
- λ_0 = length constant (Eq. 11) [m]
- $\lambda_{R_{corr}}$ = extinction length (Eq. 25) [m]
- θ = angle of scatter [rad]
- ρ_p = catalyst density [Kg m^{-3}]
- σ = volumetric scattering coefficient [m^{-1}]
- ω = latitude angle [rad]

Literature Cited

1. Cassano AE, Martin CA, Brandi RJ, Alfano OM. Photoreactor analysis and design: fundamental and applications. *Indus Eng Chem Res.* 1995; 34:2155-2201.

2. Cassano AE, Alfano OM. Reaction engineering of suspended solid heterogeneous photocatalytic reactors. *Catal Today*. 2000;58:167-197.
3. Santarelli F. Radiative transfer in photochemical processes. In: Schiavello M, ed. *Photoelectrochemistry, Photocatalysis and Photoreactors. Fundamentals and Developments*. Dordrecht: Reidel; 1985:549-559.
4. Brandi RJ, Alfano OM, Cassano AE. Modeling of radiation absorption in a flat plate photocatalytic reactor. *Chem Eng Sci*. 1996;51(11):3169-3174.
5. Romero RL, Alfano OM, Cassano AE. Cylindrical photocatalytic reactors. Radiation absorption and scattering effects produced by suspended fine particles in an annular space. *Indus Eng Chem Res*. 1997;36:3094-3109.
6. Brandi RJ, Alfano OM, Cassano AE. Rigorous model and experimental verification of the radiation field in a flat plate solar collector simulator employed for photocatalytic reactions. *Chem Eng Sci*. 1999;54:2817-2827.
7. Brandi RJ, Alfano OM, Cassano AE. Evaluation of radiation absorption in slurry photocatalytic reactors. Part II: Experimental verification of the proposed method. *Environ Sci Technol*. 2000;34(12):2631-2639.
8. Spadoni G, Bandini E, Santarelli F. Scattering effects in photosensitized reactions. *Chem Eng Sci*. 1978;33:517-524.
9. Pasquali M, Santarelli F. Radiative transfer in photocatalytic systems. *AIChE J*. 1996;42(2):532-537.
10. Brucato A, Rizzuti L. Simplified modelling of radiant fields in heterogeneous photoreactors. Part I: Case of zero reflectance. *Indus Eng Chem Res*. 1997;36:4740-4747.
11. Brucato A, Rizzuti L. Simplified modelling of radiant fields in heterogeneous photoreactors. Part II: Limiting two flux model for the case of reflectance greater than zero. *Indus Eng Chem Res*. 1997;36:4748-4755.
12. Hammersley JM, Handscomb DC. *Monte Carlo Methods*. London: Chapman and Hall Ltd.; 1983.
13. Brandi RJ, Alfano OM, Cassano AE. Evaluation of radiation absorption in slurry photocatalytic reactors. Part I: Assessment of methods in use and new proposal. *Environ Sci Technol*. 2000;34(12):2623-2630.
14. Siegel R, Howell JR. *Thermal Radiation Heat Transfer*. London: McGraw-Hill Book Company; 1972.
15. Augugliaro V, Marci G, Palmisano L, Pramauro E, Bianco-Prevot A. Kinetics of heterogeneous photocatalytic decomposition of monuron over anatase titanium dioxide powder. *Res Chem Intermediates*. 1993;19(9):839-853.
16. Li Puma G, Yue PL. A novel fountain photocatalytic reactor for water treatment and purification: modeling and design. *Indus Eng Chem Res*. 2001;40:5162-5169.
17. Yokota T, Takahata Y, Nanjo H, Takahashi K. Estimation of light intensity in a solid-liquid photoreaction system. *J Chem Eng Jap*. 1989;22(5):537-542.

Manuscript received May 17, 2006, and revision received July 27, 2006.